Magnetic signature of hydrocarbon-contaminated soils and sediments at the former oil field Hänigsen, Germany

MOTI L. RIJAL[1,2], KATHARINA PORSCH[1,3], ERWIN APPEL[1*] AND ANDREAS KAPPLER[1]

1 Center for Applied Geoscience, University of Tübingen, 72076 Tübingen, Germany (erwin.appel@uni-tuebingen.de)

2 Hetauda Campus, Institute of Forestry, Tribhuvan University, Hetauda, Nepal (moti.rijal@yahoo.com)

3 Helmholtz Centre for Environmental Research - UFZ, Department of Bioenergy, Permoserstrasse 15, D-04318 Leipzig, Germany

* Corresponding author

Received: May 18, 2010; Revised: February 8, 2011; Accepted: June 22, 2011

ABSTRACT

Magnetic properties of hydrocarbon (HC) containing soils and sediments from two sites (Site A and B) of the former oil-field Hänigsen were analyzed in order to determine whether magnetic methods can be employed to delineate HC contamination of soils and sediments. Magnetic parameters such as magnetic susceptibility and induced isothermal remanent magnetizations, as well as soil and sediment properties such as pH, iron content and water content, HC content and most probable number counts of iron-metabolizing microorganisms were determined. The magnetic concentration-dependent parameters for HC contaminated samples were 25 times higher in soils from Site A than in sediment samples from Site B. However, at Site B the magnetic susceptibility was still four times higher in comparison to lithologically similar non-contaminated sediment samples from a third Site C. Newly formed magnetite containing mainly single domain particles was responsible for the magnetic enhancement, whereas superparamagnetic grains represented only a minor component. Site A had an acidic pH compared to neutral pH at Site B, and a higher crystalline and bioavailable total iron content. Nevertheless, Site B samples contained significant numbers of both iron(II)-oxidizing and iron(III)-reducing microorganisms indicating that microbial iron cycling might have taken place at this site and potentially played a role for iron mineral transformation, including magnetite (trans)formation. The content of total non-polar hydrocarbons (TNPH) at Site A was one order of magnitude higher than at Site B. Only at Site A magnetic susceptibility correlated well with TNPH. Our results demonstrate that HC contaminated samples had an enhanced magnetite content compared to non-contaminated soils and sediments. Therefore, magnetic methods may provide a quick and cost-effective way to assess HC contamination in soils and sediments. However, more field sites and laboratory investigations are needed to reveal the complex nature of the processes involved.

Keywords: magnetic properties, magnetic methods, environmental magnetism, hydrocarbon contaminated soil and sediment, iron redox cycling

1. INTRODUCTION

Pollution of soils, sediments and groundwater by organic contaminants is an important global environmental problem. In order to analyze HC contaminated sites and apply suitable remediation, rapid and cost-effective assessment methods are needed. Environmental magnetic methods have a high potential to serve as such a screening and monitoring tool for soil, water and air pollution, since they are fast and highly sensitive (*Petrovský and Ellwood, 1999*). In recent years, these methods have been well established to study heavy metal pollution in soils from different anthropogenic sources (*Evans and Heller, 2003*). Specifically, magnetic susceptibility was successfully applied to detecting anthropogenic pollution caused by fly ashes from power plants (*Kapička et al., 2000*; *Spiteri et al., 2005*; *Davila et al., 2006*), metallurgical dusts (*Hanesch and Scholger, 2002*) and urban airborne particulates (*Muxworthy et al., 2001*; *Gautam et al., 2005*). During combustion, the oxidation of material that contains a relatively large amount of iron and heavy metals (such as Pb, Cu and Zn) leads to the formation of magnetic particles. This link between heavy metals and magnetic particles explains the significant relationship between enhanced magnetic susceptibility of soils and their combustion-related pollution with heavy metals around industrial sites (*Strzyszcz and Magiera, 1998*; *Kapička et al., 1999*; *Hanesch and Scholger, 2002*).

However, there are only a few studies in which a relationship between magnetic properties and organic contaminants was studied in the environmental context. *Hanesch and Scholger (2002)* observed a correlation between magnetic susceptibility and polycyclic aromatic hydrocarbons (PAHs) content in soil near Donawitz steel mill at Leoben, Austria. After analyzing sediment cores from Hamilton harbour, Canada, *Morris et al. (1994)* concluded that magnetic susceptibility could be a reliable and less expensive empirical method for determining the extent of the contamination of sediments by PAHs. *Martins et al. (2007)* verified a good correlation between the distribution of magnetic susceptibility and hydrocarbons in the Santos Estuary, Brazil, mainly by comparing magnetic susceptibility and PAHs. Some studies have also been published investigating a possible use of magnetic properties for oil prospecting and exploration. *Liu et al. (2006)* reported magnetic enhancement that was caused by HC migration in the Mawagmiao Oil Field, Jianghan Basin, China. The authors observed a dramatic increase of some magnetic parameters such as magnetic susceptibility and saturation magnetization of an oil-bearing formation and also observed the presence of secondary magnetite particles in association with the oil-bearing strata. A study done by *Aldana et al. (2003)* in oil reservoirs in Venezuela demonstrated that high-resolution aeromagnetic survey can be applied for exploring oil fields, suggesting that magnetic susceptibility measurements in soils, sediments, and drill cuttings may be a complementary or alternative method for exploration and assessment of HC reservoirs. *Díaz et al. (2006)* used magnetic susceptibility, electron paramagnetic resonance and extractable organic matter parameters in drilling fines from near surface levels of producer and non-producer wells to examine a possible causal relationship between magnetic anomalies and underlying hydrocarbons. In a recent study *Guzmán et al. (2011)* argued that magnetic susceptibility together with other non-magnetic parameters could be used for preliminary reservoir characterization. *Aldana et al. (2011)* showed that magnetic mineralogy associated to hydrocarbon

microseepage in oil fields of western Venezuela is represented by magnetite. Magnetic properties changes were also recognized in the groundwater table fluctuation zone of HC contaminated sediments (*Rijal et al., 2010*). In several of these studies, correlation of magnetic susceptibility with organic compounds might be a secondary feature as heavy metal input appears together with enhanced magnetic susceptibility and organic compounds are likely abundant as an additional contaminant. In any case, the controlling factors of magnetic property changes in soil and sediments in the presence of organic contaminants are still poorly understood.

Some iron(III)-reducing microorganisms can use hydrocarbons as a carbon source to reduce iron(III) to iron(II) (*Lovley et al., 1989*; *Lovley and Anderson, 2000*), which in turn can be oxidized by anaerobic and aerobic iron(II)-oxidizing bacteria (*Kappler and Straub, 2005*; *Weber et al., 2006*). Both microbial iron(III) reduction and iron(II) oxidation can lead to the formation of magnetite (*Bazylinski et al., 2007*). HC contaminations in soils and sediments, therefore, have an influence on both iron(III)-reducing and iron(II)-oxidizing microorganisms and thereby on iron mineral (trans)formation and dissolution processes. These processes can lead to changes in the magnetic iron mineral content of soils and sediments. Magnetic properties, mainly magnetic susceptibility, can be measured very quickly and in a cost-effective way to study or monitor such changes of magnetic iron mineral contents in contaminated soils and sediments.

Assuming that the change in magnetic iron mineralogy in HC contaminated soils and sediments can be caused by biological as well as abiological processes, our main hypothesis was that magnetic methods can be used to investigate and monitor such iron mineralogical changes. Therefore, the main goals of this study were: (i) to determine if magnetic parameters of HC contaminated soils and sediments change due to HC contamination in comparison to non-contaminated areas, and (ii) to investigate the role of sediment and soil parameters, such as pH and total iron content, which might also influence the microbial iron cycling and thereby change magnetic properties in the presence of hydrocarbons. We report results obtained from the HC contaminated field site Hänigsen, northern Germany, which represents an area where hydrocarbons are the only contaminants and anthropogenic heavy metal input can be neglected.

2. MATERIALS AND METHODS

2.1. Field Sampling

The study area, Hänigsen (52°28′58″N, 10°5′47″E) is located approximately 100 km north of Hannover in northern Germany (Fig. 1a). Salt tectonics in the northern German basin has led to natural oil outcrops at the surface, which have been exploited for more than 400 years on a small scale by collecting oil in one to two meter deep pits. The area around Hänigsen led to intensive modern oil exploitation by drilling and later also by underground mining for oil-bearing sand during the oil boom in the 1920s. Oil production and processing around these areas continued until 1963 with about 2000 production wells.

Several HC contaminated samples of forest soil and of sediments from two different locations (sites A and B) were collected in the Hänigsen area. In addition to these contaminated samples, two samples were collected from a non-contaminated site (Site C) as background material for the comparison of its magnetic properties with those of the

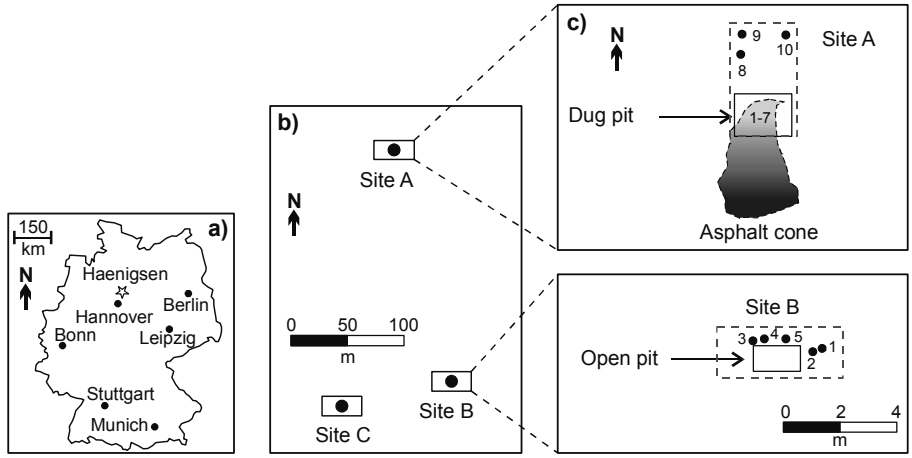

Fig. 1. **a)** Location map of the study site; **b)** sampling layout of the three different sampling Sites A, B, C; **c)** distribution of sampling points within the two contaminated sampling Sites A and B; non-contaminated samples were taken from two different depths at Site C.

contaminated samples. The location of all three sites is shown in Fig. 1b and 1c, and the depth of the samples is presented in Table 1.

The HC contaminated samples from Site A were mainly soil samples taken from maximum 0.85 m depth, whereas at Site B sediment samples were taken from 1.8 to 2.4 m below the soil surface. Site A is a dried oil-leaking surface while Site B is a former oil-pit maintained by local people for historical demonstration purposes.

The samples from Site B were water-saturated and taken from beneath the groundwater table. The individual samples from sites A and B were located within a lateral distance of 1.5 and 2 m to each other, respectively. Samples from the non-contaminated sediments at Site C were collected from a maximum of 0.9 m below the surface. All samples were stored in plastic bags and kept at 4°C until subsequent measurement.

2.2. Laboratory Sample Characterization

2.2.1. Magnetic Measurements

Mass-specific magnetic susceptibility (χ), frequency-dependent magnetic susceptibility ($k_{FD\%}$), temperature dependence of magnetic susceptibility k, anhysteretic remanent magnetization (*ARM*) and isothermal remanent magnetization (*IRM*) were measured after drying the samples at room temperature. Five sub-samples of each sample from all sites were packed into 10 cc plastic containers. k was measured with a KLY-3 Kappabridge (AGICO) at room temperature. $k_{FD\%}$ was obtained with a Bartington dual frequency MS2B sensor at two different frequencies (470 and 4700 Hz). *ARM* was induced with a steady biasing field of 40 μT and a peak alternating field of 100 mT using a Model 615 ARM magnetizer (2G Enterprises). *IRM* was imparted with a MMPM9 pulse magnetizer by exposing samples to a series of successively larger fields starting from

Table 1. Sampling depths, pH values, water content, Fe_{cryst} and Fe_{bio} of the sampling sites.

Sampling Site	Sample Label	Depth [m]	pH	*WC* [%]	Fe_{cryst} [%]	Fe_{bio} [%]
A	A1	0.25–0.30	2.8	19.60	13.86	3.49
	A2	0.30–0.35	4.6	15.70	14.36	1.26
	A3	0.40–0.50	6.7	9.87	11.12	1.36
	A4	0.00–0.05	3.9	11.70	17.18	0.82
	A5	0.05–0.10	3.8	34.80	16.98	2.58
	A6	0.10–0.15	4.5	10.70	11.88	0.87
	A7	0.80–0.85	3.3	32.20	10.00	0.92
	A8	0.00–0.05	3.4	7.50	3.36	0.65
	A9	0.05–0.10	3.8	10.70	31.70	2.83
	A10	0.10–0.20	6.7	15.60	7.09	2.59
B	B1	1.80–2.15	6.7	Water saturated samples	5.39	0.41
	B2	2.15–2.40	6.9		8.54	1.43
	B3	1.80–2.10	6.6		4.69	0.41
	B4	2.30–2.40	7.3		10.43	1.34
	B5	2.00–2.20	7.4		10.15	2.03
C	C1 C2	not measured				

10 mT to 1 T, regarded as the saturation *IRM* (*SIRM*), followed by successively larger backfields up to −300 mT remanent magnetizations (*ARM* and *IRM*) were measured using a Minispin magnetometer (Molspin Ltd.). *S*-ratios (after *Bloemendal et al., 1992*) for −100 and −300 mT fields and *ARM*/*SIRM* ratios were calculated to distinguish magnetic mineral phases and their grain size (more precisely, magnetic domain state).

For identification of the magnetic mineralogy and magnetic grain size, low temperature remanence was recorded in some samples selected from sites A, B and C. The measurement was performed with a magnetic property measurement system (MPMS) by warming the samples from 10 to 300K starting from an initial state after applying a saturating field of 2.5 T (zero-field cooling: ZFC). Some representative samples from all three sites were demagnetized by applying a 2.5 T field at room temperature (*RT*) and then cooling from 300 to 10K (*RT SIRM* cooling). In addition, the mineralogical content of a selected sample from Site A was also examined by measuring temperature dependence of *k* with a KLY-3 Kappabridge by heating the samples from room temperature to a maximum of 700°C.

2.2.2. Soil and Sediment Characterization

The pH, water content (*WC*), total crystalline iron (Fe_{cryst}) and bioavailable iron (Fe_{bio}) content were determined to characterize the soil and sediment samples, and to investigate their relationship with their magnetic properties.

After sample collection, soils were stored in plastic bags in darkness at 4°C until further use. Some samples were highly contaminated with crude oil and therefore impossible to sieve. In order to treat all soil and sediment samples in the same way large

particles (e.g. stones, roots) were removed from all samples by hand with tweezers before further analysis. Soil water content was determined and calculated after standard protocols (*Blume et al., 2000*). The pH was measured 24 h after addition of 25 ml of 0.01 M $CaCl_2$ solution to 10 g of soil (*Blume et al., 2000*). Two different iron fractions, "bioavailable iron" (Fe_{bio}) and crystalline iron minerals (Fe_{cryst}), were extracted independently of each other with a soil/extractant ratio (w/v) of 1:50 and with at least 0.5 g of field moist soil (*Moeslund et al., 1994*; *Roden and Zachara, 1996*). Adsorbed iron, iron carbonates and poorly crystalline iron minerals, so called Fe_{bio} were extracted with 0.5 M HCl at room temperature with continuous agitation for 1 h on a shaker. Fe_{cryst} was extracted with 6 M HCl at 70°C in a water bath for 24 h and the extracts were cooled for 15 min at room temperature. 1.8 ml of each extract was centrifuged for 15 min at 20.817 g to remove soil particles. The total iron in the supernatants was quantified by the ferrozine assay and the concentration was corrected by the water content of the respective samples (*Stookey, 1970* and *Hegler et al., 2008*). Pb and Zn contents of finely ground soil dried at 105°C were quantified by X-ray fluorescence analysis (Bruker AXS S4 Pioneer X-ray spectrometer, Bruker AXS GmbH, Germany).

2.2.3. Hydrocarbon Analysis

The HC content of samples from sites A and B was measured after extracting well homogenized 10 g of moist sample with two solvents: first with acetone and subsequently with florisil. The second solvent, florisil was added to remove polar compounds because these compounds are sticking on the gas chromatography column and can therefore not be measured accurately. Afterwards, the extract was analyzed by gas-chromatography mass-spectrometry (GC-MS) (HP 6890-II and MS 5973). HC were identified by matching retention times and ion mass fragments with results from standard mixtures of diesel and mineral oil (both without additives) (DIN H53). The remaining HC content can be referred as total non-polar hydrocarbon (*TNPH*) content including PAHs. The following types of PAHs were quantified with a GC-MS: Naphthalene, 2-Methylnaphthalene, 1-Methylnaphthalene, Acenaphtylene, Acenaphtene, Fluorene, Phenanthrene, Anthracene, Fluoranthene, Pyrene, Benzo (a) anthracene, Chrysene, Benzo (b) fluoranthene, Benzo (k) fluoranthene, Benzo (a) pyrene, Indeno (1,2,3-cd) pyrene, Dibenzo (ah) anthracene and Benzo (ghi) perylene. The sum of these PAHs was calculated and this parameter was called total PAH (*TPAH*) content.

2.2.4. Most Probable Number (*MPN*) Counts

Viable anaerobic, mixotrophic nitrate-reducing iron(II)-oxidizing microorganisms (FeOxM) and viable anaerobic iron(III)-reducing microorganisms (FeRedM) present in sediment samples B1, B3 and B5 were quantified by the most probable number (*MPN*) method (*Cochran, 1950*). Dilution series of sediment suspensions were set up with selective growth medium for the two metabolic groups of microorganisms (supporting information S1). Based on the number of parallels per dilution step showing growth after 17 weeks, the *MPN* of cells per gram of sediment present in the initial sediment sample was calculated with the program "Most Probable Number Calculator" version 4.04 (Environmental Protection Agency, USA) and corrected after *Salama et al. (1978)* as described by *Klee (1993)*. The cell numbers were corrected by the water content of the soil.

3. RESULTS

3.1. Magnetic Characteristics

3.1.1. Concentration of Magnetic Phases

First, as a remarkable result, we found that near surface (< 1 m depth) contaminated samples from Site A had a very high χ, with mean values nearly 25 times higher than sediment samples from deeper depth at Site B (Fig. 2a and b, Table 1). Furthermore, the variability of χ among the samples A1–A7 from Site A were larger than the variability of χ among samples from Site B. Samples A1–A7 which were sampled just below the asphalt cone had a higher χ in comparison to samples A8–A10 that were located further away from it. The sediment samples from Site B exhibited $\chi < 10 \times 10^{-8}$ m^3/kg as indicated in Fig. 2b. The average χ of all samples from Site B, however, was still more than four times higher than the average χ of non-contaminated samples taken from Site C ($\chi = 1.06 \times 10^{-8}$ m^3/kg).

There is a strong linear relationship between χ and *ARM*, which shows that χ at both sites A and B is mainly controlled by ferro(i)magnetic particles (Fig. 3a and b). These samples do not contain a large amount of superparamagnetic grains as depicted by the very low $k_{FD\%}$ (< 3%) (Fig. 3c and d). There is no significant relationship between χ and $k_{FD\%}$ at both sites.

3.1.2. Magnetic Mineral Characterization

Volume magnetic susceptibility k was measured during heating sample A6 up to 700°C to determine the type of ferro(i)magnetic minerals present. New formation of magnetite during heating masks the results (Fig. 4). k showed upon heating a plateau-like behaviour with significant positive values below 400°C. At higher temperatures, new formation of magnetite, probably caused by oxidation of pyrite (e.g. *Krs et al., 1992*; *Liu et al., 2004*; *Chang et al., 2008*) masks the results. The slight increase of k around 250°C could be either due to the formation of maghemite and its destruction at 300–400°C

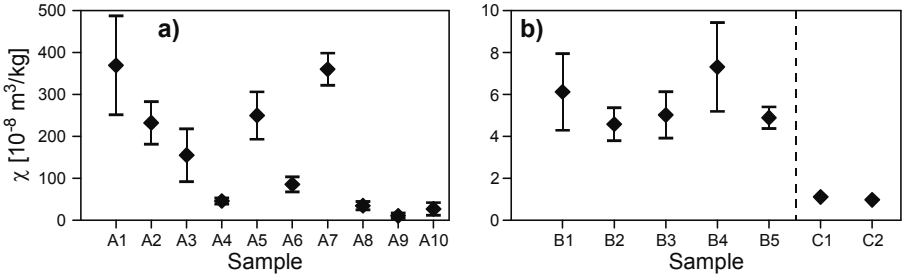

Fig. 2. Plots of mass-specific magnetic susceptibility χ mean values: **a)** samples from sampling Site A, **b)** samples from Sites B and C. Five sub-samples from each sample were measured. Each data point is the mean of the five sub-samples. The error bars are shown. The sample name is shown along the horizontal axis.

(slight decrease of k) or due to fine particles which are single domain (SD) at room temperature and become superparamagnetic at increasing temperature.

ZFC curves revealed a 65% loss of remanence between 30K and 130K (Verwey transition ~120K and magnetocrystalline isotropic point of magnetite ~130K) for the contaminated sample A6, whereas for the non-contaminated sample C2 this loss is 95%

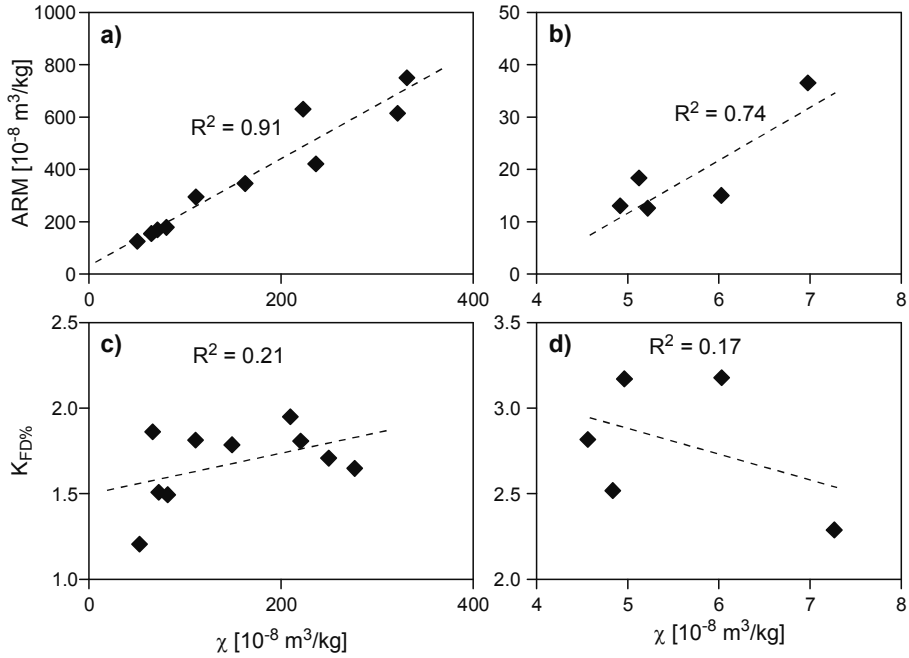

Fig. 3. Linear scatter plots of mean values of: **a)** *ARM* and χ of samples from Site A; **b)** *ARM* and χ of samples from Site B; **c)** $k_{FD\%}$ and χ of samples from Site A; **d)** $k_{FD\%}$ and χ of samples from Site B. The dashed lines show the best linear fit, R^2 denotes the coefficient of determination.

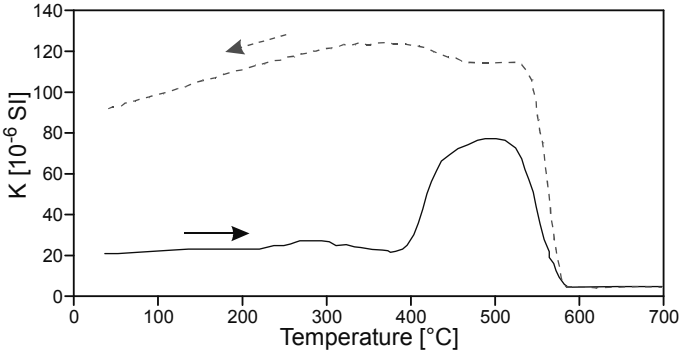

Fig. 4. Temperature dependence of magnetic susceptibility k of sample A6. The sample was measured after extraction of hydrocarbons.

and the Verwey transition is weakly expressed (Fig. 5a). For *RT*, *SIRM* of Site A samples revealed a clear effect at the Verwey transition. For sites B and C samples the Verwey transition is visible but less prominent (Fig. 5b).

The magnetic granulometry indicator ratio was plotted *ARM*/*SIRM* versus χ for both sites A and B (Fig. 6a and b). *ARM*/*SIRM* was positively correlated with χ for the samples from Site B ($R^2 = 0.79$) indicating new formation of predominantly SD magnetite particles in contaminated samples. There was no such relationship between *ARM*/*SIRM* and χ for the samples from Site A. However, the *ARM*/*SIRM* ratios were similar to that of samples from Site B. This indicates that at Site A a significant amount of SD magnetite has also been formed. The S_{-100} around 0.90 indicates that soft magnetite dominates in all contaminated samples (Fig. 6c). All contaminated samples yield S_{-300} around 0.95 indicating that these samples were dominated by magnetite, whereas clean samples showed a mean S_{-300} below 0.90, suggesting that a hard magnetic phase-like hematite was more predominate than magnetite.

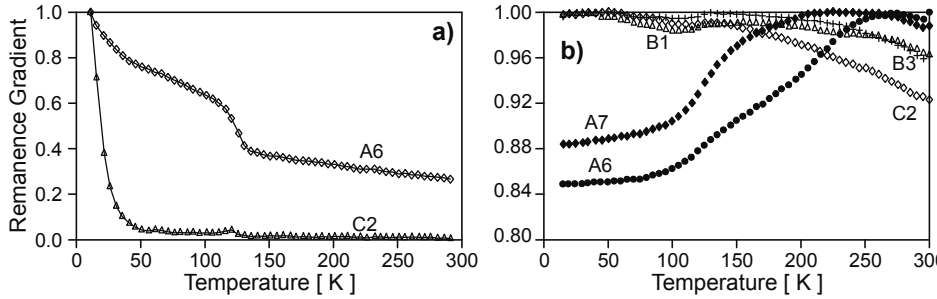

Fig. 5. Normalized gradient of low-temperature magnetic remanence for representative samples from the contaminated Sites A and B and the non-contaminated Site C. **a)** Zero-field cooling, **b)** room-temperature remanence cooling.

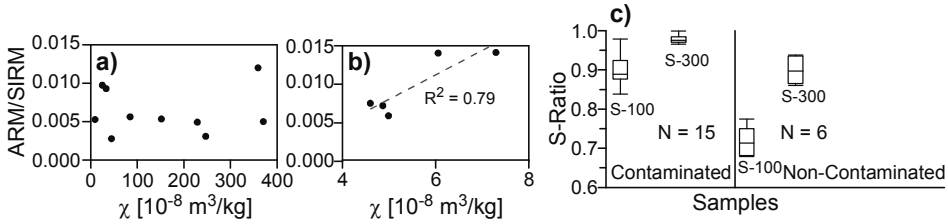

Fig. 6. Linear scatter plots of *ARM*/*SIRM* ratio vs. χ of samples from: **a)** Site A and **b)** Site B; the line in **b)** indicates the best linear fit between these two parameters and R^2 denotes the coefficient of determination. **c)** *S*-ratio for backfields of −100 and −300 mT of all measured samples from contaminated (A and B) and non-contaminated (C) sites calculated after *Bloemendal et al. (1992)*; *N* means the total number of samples measured from contaminated Sites A and B, and non-contamianted samples from Site C (including sub-samples).

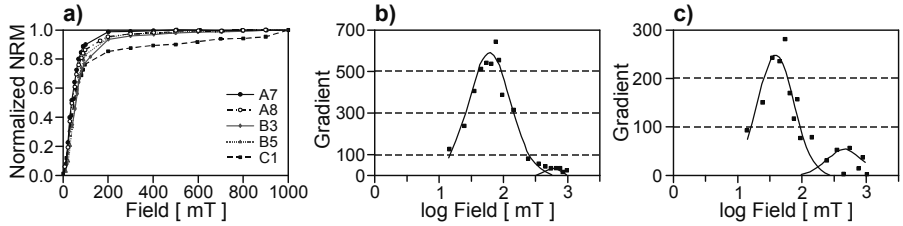

Fig. 7. **a)** Normalized *IRM* vs. applied field for selected samples from sites A, B and C. **b)** Decomposition of *IRM* acquisition curves of contaminated sample B3 and **c)** non-contaminated sample C1 after *Kruiver et al. (2001)*.

The linear *IRM* acquisition depicts that the contaminated samples from both sites (A7, A8, B3, B5) saturated around 300 mT whereas the non-contaminated sample (C1) was not fully saturated at 1 T (Fig. 7a). Log-normal Gaussian coercivity spectra (after *Kruiver et al., 2001*) were modeled for a two component system. The results showed that contaminated samples (Fig. 7b) were dominated by a soft magnetic component (contribution 98%, mean $B_{1/2}$ of 50 mT) whereas the non-contaminated samples (Fig. 7c) had a significant additional contribution (20%) of a harder coercivity phase ($B_{1/2}$ of several 100's mT) probably related to hematite.

3.2. Soil and Sediment Properties

The mean water content (*WC*) at Site A was 17%, whereas at Site B the samples were water saturated. The mean pH was almost neutral (≈ 7) at Site B, whereas most of the samples from Site A had an acidic pH value (≈ 4). The averaged Fe_{cryst} content of samples from Site A was about 1.70 times higher than for samples from Site B (average of 13.1 and 7.8wt.% for Fe_{cryst}, respectively) while the averaged Fe_{bio} content was only slightly higher for A than for B samples (average of 1.7 and 1.1wt.% for Fe_{bio}, respectively) (Table 1). The difference between the content of Fe_{bio} and Fe_{cryst} within the study sites could have mostly caused by the nature of soils and sediments properties, hydrocarbon contamination and microbial transformations of iron minerals.

3.3. Most Probable Numbers of Fe(II)-Oxidizing and Fe(III)-Reducing Microorganisms

In order to determine how many microorganisms which are directly involved in the iron cycling under anoxic conditions were present at Site B, the numbers of anaerobic FeRedM and FeOxM in sample B1, B3 and B5 were determined by the *MPN* method (Fig. 8).

Both metabolic groups of microorganisms were found in all three samples. Among the samples the cell numbers of both groups varied between 4×10^2 and 4×10^6 cells per gram dry soil, with the lowest cell numbers being enumerated in sample B3 and the highest in sample B5. In all three samples, the number of FeRedM was similar to the number of FeOxM.

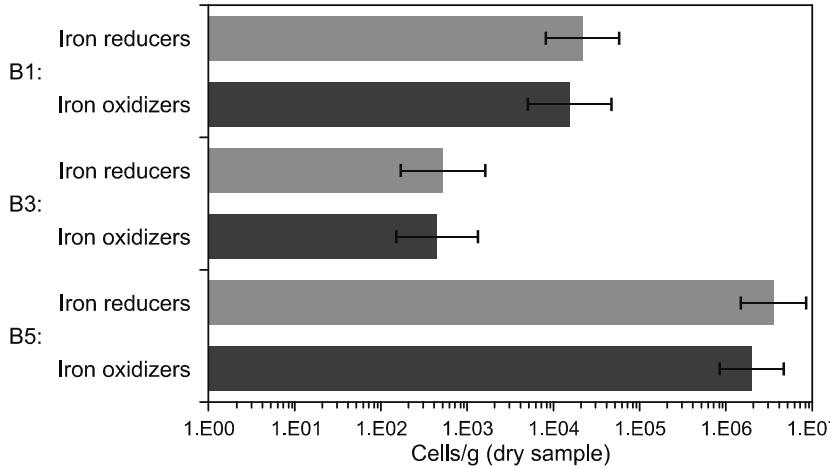

Fig. 8. Cell numbers of viable anaerobic iron(III)–reducing microorganisms (FeRedM) (light bars) and anaerobic, mixotrophic nitrate-reducing iron(II)-oxidizing microorganisms (FeOxM) (dark bars) in Samples B1, B3 and B5, quantified by the most probable number method. Error bars indicate the 95% confidence interval.

3.4. Relationship between Magnetic and Non-Magnetic Parameters

There was a very strong relationship ($R^2 = 0.85$) between χ and *TNPH* for Site A (Fig. 9a). However, the relationship between χ and *TPAH* was very weak. These results probably suggest that *TNPH* provided easily available carbon sources for microorganisms, which lead to new formation of magnetite. The values of *TNPH* and *TPAH* at Site B were one order of magnitude lower than at Site A. In contrast, the samples from Site B showed neither a correlation between χ and *TNPH* nor between χ and *TPAH*.

The relationship among magnetic parameters, non-magnetic parameters and the HC content of all samples was defined by hierarchical cluster analysis using SPSS 11.5. The analysis was performed using the medians of nine different variables (χ, *ARM*, $k_{FD\%}$, pH, *WC*, *TNPH*, *TPAH*, Fe_{cryst}, Fe_{bio}) obtained for all samples from sites A and B. All nine variables were grouped together using Pearson correlation as a grouping criterion of different variables (Fig. 10). The dendrogram showed that the magnetic concentration parameters χ and *ARM* are closely related to the contents of *TNPH*. All other relationships are weak.

4. DISCUSSION

Soil samples from Site A were mainly samples that were situated very close to a source of HC contamination, the dried oil-leaking surface. These samples were also located close to the soil surface and had a significant higher χ than the samples from Site B which were sampled from a deeper contaminated water saturated zone. Differences

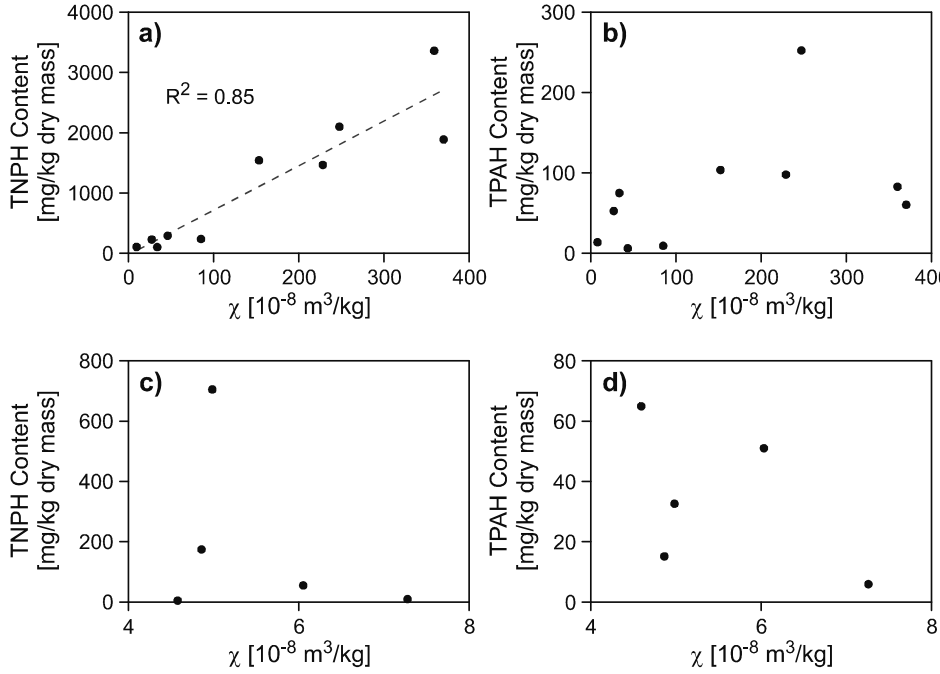

Fig. 9. Linear scatter plots of: **a)** *TNPH* content from Site A (the regression line indicates the best linear fit, R^2 denotes the coefficient of determination), **b)** *TPAH* content from Site A, **c)** *TNPH* content from Site B, **d)** *TPAH* content from Site B as a function of mass-specific magnetic susceptibility χ.

in χ (Fig. 2) could be due to the variability of natural soil, differences of HC contents, redox zonations and/or variable pH (2.8–7.4) conditions. In contrast to Site B, the dried oil-leaking surface at Site A might have played a significant role for an increase of magnetic properties by forming a partially closed system, which diminished free exchange of fluids with its sorroundings. One of the reasons of magnetically enhancement in soil may be due to conversion of some weakly magnetic iron oxides or other iron source into strongly magnetic phases as magnetite and maghemite (*Maher, 1998*). More than 30 species of iron(III)-reducing soil microorganisms have been identified (*Fischer, 1998*; *Rossello-Mora et al., 1995*). Such microorganisms may play a key role in pedogenic formation of ultrafine-grained magnetite by production of Fe^{2+} ions (*Maher, 1991*). In certain conditions, the interaction between the formed Fe^{2+} and ambient Fe^{3+} ions may result in inorganic precipitation of magnetite (*Lovley et al., 1987*).

It was noted that at low pH (3.0–4.0), dissolution of ferro(i)magnetic minerals is more likely than their neoformation (*Grimley et al., 2004*). Our results (high χ of samples from an acidic and contaminated environment, Site A) did not support these findings, but indicated that the formation rather than the dissolution of magnetic minerals occurred when a large amount of carbon source in the form of hydrocarbons was available. It was also noticed by *Grimley and Arruda (2007)* that the dissolution of strongly magnetic

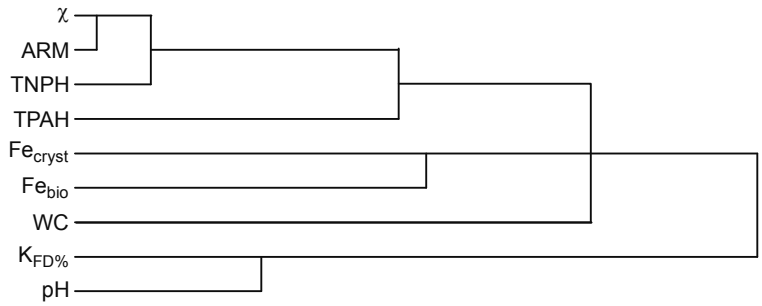

Fig. 10. Dendrogram of nine different variables obtained from ten samples from Site A and five samples from Site B. Variables are grouped together using median method and Pearson correlation as grouping criterion.

minerals is a common and relatively rapid phenomenon in poorly drained soils, which results in low χ values.

Samples from Site B, which were mainly sediment samples that laid about at least 1.8 m below the soil surface and remained water saturated throughout the year, had a much smaller χ in comparison to samples from Site A. *Maher et al. (1986)* showed that soils that are seasonally saturated with water and reduced in iron have lower χ values than soils that are better drained and not iron-reduced. Depletion of magnetic minerals is especially prevalent in strongly reduced, anoxic soils in the presence of organic matter (*Maher, 1986, 1998*). Also, *Grimley and Arruda (2007)* observed that at low E_h the reducing conditions are primarily responsible for magnetic mineral dissolution, a process likely mediated by FeRedM in the presence of soil organic matter. They also mentioned that although experiments indicate that reductive dissolution of magnetite can occur abiotically under extreme conditions, microorganisms likely play an important role in the natural environment. Their findings also supported our results because both FeRedM and FeOxM were present in samples from Site B, where samples were water-saturated and the χ signal was lower than at Site A. Nevertheless, samples from Site B had more than three to four times higher χ than the lithologically similar sediment samples from the non-contaminated Site C, suggesting that HC contamination was responsible for the observed increase of χ. Therefore, the highest χ at Site A could have been caused by both higher HC concentration and microbial transformation of iron minerals.

In order to rule out a significant influence of atmospheric heavy metal input (and therefore magnetic enhancement as known from previous studies) in the near-surface sample A5 from Site A, the metal content was examined by X-ray fluorescence (XRF). The Pb and Zn contents in this sample were 82 and 50 ppm, respectively. This might reflect some anthropogenic contamination; however, the heavy metals content is clearly lower than the observed at contaminated sites like those around steel industry sites, Leoben, Austria (*Blaha U., University of Tuebingen, personal communication, 2004*). The sediment samples from Site B did not contain any significantly enhanced heavy metal levels. As these samples were taken from deeper depths, anthropogenic input by atmospheric deposition was unlikely. Magnetic enhancement in relation to anthropogenic

heavy metal contamination might be responsible for part of the high χ values at Site A, but certainly did not explain the increased χ values of samples from Site B compared to the non-contaminated samples from Site C. It is likely that the samples from Site B had a lower magnetic mineral concentration than those of Site A because these samples were completely water saturated, which favors dissolution of magnetic grains or suppresses new formation of magnetite (*Rijal et al., 2010*).

Mineral magnetic parameters demonstrate that the magnetic enhancement was due to magnetite. Remanence parameters (*ARM* and *SIRM*) as well as χ were dominated by the magnetite phase. There were almost no ultrafine-grained superparamagnetic particles present as denoted by very low $k_{FD\%}$ values of samples from both contaminated sites (Fig. 3). The positive correlation of *ARM*/*SIRM* and χ indicates that the newly formed magnetite contains a significant portion of SD particles because *ARM* is mainly acquired by SD particles in magnetite. Such correlation is missing in samples from Site A, however, the *ARM*/*SIRM* ratios were similar to Site B samples. Therefore, it can be concluded that also at Site B newly formed magnetite was at least partly in the SD range. The increased χ at both sites is likely caused mostly by SD magnetite of biogenic origin. The presence of SD magnetite particles in ground water table fluctuation zones of HC contaminated areas was already demonstrated by *Rijal et al. (2010)*.

A positive relationship between *TNPH* and χ is evident for Site A (Fig. 9). The *TPAH* content, however, did not correlate with χ ($R^2 = 0.20$). Water-saturated samples from Site B did not show any clear relationship of HC content with χ. The *TNPH* and *TPAH* content was about one order smaller at Site B compared to Site A. This could be explained by a larger mobility of HC phases within the groundwater leading to a faster removal from this zone. The residence time of HC at Site B, however, is probably long enough to enable new formation of magnetite due to microbial activity. Due to mobility, the *TNPH* concentration might have been much higher at an earlier time, even leading to toxic effects for microorganism. These scenarios may explain why magnetic mineral concentration was enhanced at Site B compared to the non-contaminated Site C, but was without any noticeable correlation of χ with actual *TNPH* contents. The samples from Site A had higher total crystalline and bioavailable iron contents than samples from Site B. At Site B, the water-saturated condition might have led to an outwash of fine iron particles from this site and hence to a lower total iron content. The dissolution of magnetic minerals in water saturated soil samples was also noticed by *Grimley and Vepraskas (2000)*. Furthermore, there might be a difference in iron mineral (trans)formation processes in HC contaminated soils/sediments with and without water saturation, which might play an important role for creating such differences in the total bioavailable iron content. However, despite the lower iron content at the contaminated Site B, *MPN* measurements showed that both FeOxM and FeRedM are present in samples from this site. Under iron(III)-reducing conditions, the degradation of organic contaminants such as aromatic hydrocarbons can be directly coupled to microbial iron(III) reduction (*Lovley and Anderson, 2000*). Similar cell numbers for FeRedM as for our Site B samples were determined by the *MPN* method in the iron reduction zones of gasoline contaminated soils 10^3 cells/g soil (*Kao et al., 2001*) and in crude oil contaminated aquifer sediments 10^4–10^6 cells/g sediment (*Bekins et al., 1999*).

On the other hand, iron(II) formed by microbial iron(III) reduction under anoxic conditions can be used by anaerobic FeOxM (*Kappler and Straub, 2005*). The similar cell numbers of FeOxM and FeRedM in our samples suggest that FeOxM were stimulated/influenced by the geochemical conditions to the same extent as the FeRedM. Microbial cycling of iron under anoxic conditions coupled to the complete oxidation of benzoate was shown by *Straub et al. (2004)*. Hence, also at Site B microbial cycling of Fe associated with the degradation of hydrocarbons might have occurred. Furthermore, aerobic Fe(II)-oxidizers could be coupled to Fe(III) reduction at oxic-anoxic interfaces and thereby to the degradation of hydrocarbons.

5. CONCLUSIONS

The present study performed with HC contaminated soils and sediments from the former oil field in Hänigsen revealed that there is a reasonable relationship between the enhancement of magnetite concentration and the content of hydrocarbons in soils, in particular *TNPH* at Site A. Similar *ARM*/*SIRM* at both sites suggest that the same processes also affects Site B sediments, but water saturation may lead to magnetite dissolution and HC mobilization, explaining the lack of correlation between χ and *TNPH* at Site B. FeOxM and FeRedM were present and might have played an important role in the (trans)formation of iron minerals in HC contaminated sediments, and probably in Site A soils. Newly formed magnetite had a significant contribution in the single domain grain size range. The relationship between HC content and magnetic parameters was not quite clear in the case of HC contaminated sediment samples. The significant increase of magnetic concentration parameters in Site B compared to the non-contaminated nearby Site C, with similar lithology, suggests the formation of magnetite in HC contaminated sediments. The similarity of *ARM*/*SIRM* ratios at both HC contaminated sites reveals that there was neo-formation of magnetite at Site A, though it has different lithology than Site B.

High mobility of hydrocarbons, as well as magnetite dissolution or suppression of magnetite formation due to water saturation, might explain the lack of direct correlation between magnetic concentration and *TNPH* at Site B. We concluded from our results that HC contamination can be delineated by measuring magnetic proxy parameters. However, the processes relating HC and magnetic properties are complex and more field and laboratory studies are required to evaluate the variability and general characteristic effects of HC on magnetic properties of soils and sediments.

APPENDIX
MOST PROBABLE NUMBER (MPN) OF FeOxM AND FeRedM

All labware used during this procedure was sterile, and all solutions were sterile and anoxic. For sample B1, B3 and B5, 1 g of soil was suspended in 2.5 ml (B5) and 5 ml (B1, B3) of 0.09% NaCl solution in a 20 ml glass vial with N_2 atmosphere. Since sample B3 and B5 could not be suspended due to their very high crude oil content, two sterile glass beads were added to the vials to facilitate removal of cells from the soil and the samples were horizontally shaken for 6–7 days. The soil suspension was consecutively diluted

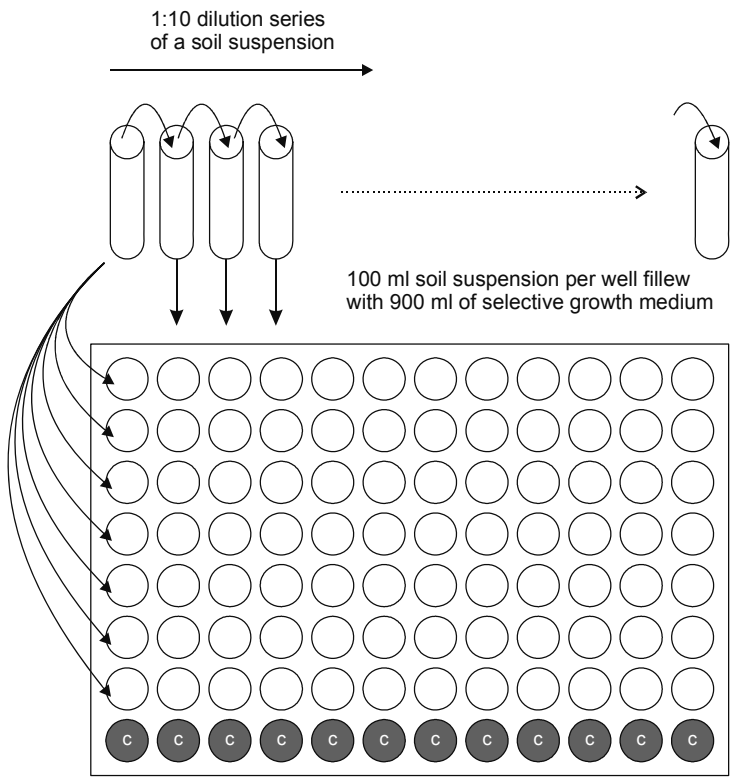

Fig. A1. Set-up to quantify cell numbers of FeOxM and FeRedM in 96 well plates by the most probable number method with a dilution series of 12 dilutions and 7 parallels. The last row of the plate serves as sterile negative control.

eleven times 1:10 with freshwater medium (see below) to obtain a dilution series of 12 dilutions. Per targeted microorganism group and soil sample, a 96 well plate was filled with selective growth medium (see below) in a glovebox (100% N_2) and from each of the 12 dilution 100 µl were added to each well of one single column except the last well (Fig. A1). By increasing the dilution from the left to the right of the plate, twelve 1:10 dilution steps each with seven parallels were obtained. The last row of the plate served as sterile negative control. The plates were sealed with a sterile polyester foil (Roth) and incubated in airtight plastic incubation bags with an oxygen-removing and CO_2-producing unit (Anaerocult®A mini, Merck) in the dark at 20°C for 17 weeks. The *MPN* of cells in a sample is statistically calculated based on the number of parallels of a 1:10 dilution series showing growth. For plates containing FeOxM selective media, positive wells were identified by a color change from white to greenish-gray. For the FeRedM plates a ferrozine assay (*Stookey, 1970*) of one aliquot per well was performed and wells with twice as high iron(II) concentration than the average iron(II) concentration of the control wells were counted as positive.

The vitamins and trace elements containing freshwater medium (*Straub et al., 2005*) was buffered to pH 7.2 with 30 mM $NaHCO_3$ and used with a headspace of N_2:CO_2 (90:10). The selective growth medium of the FeOxM consisted of freshwater medium with 10 mM $FeCl_2$, 4 mM $NaNO_3$ and 0.5 mM Na-acetate. For the selective growth medium of the FeRedM, the freshwater medium contained 5 mM ferrihydrite and the following electron donor mixture: 5 mM Na-acetate, 5 mM Na-lactate, 10 mM Na-formate, 2 mM Na-propionate and 2 mM Na-butyrate. The ferrihydrite was synthesized according to *Raven et al. (1998)*, but was washed with water instead of NaCl solution.

Acknowledgements: We would like to thank U. Blaha for his help during field sampling, T. Wendel for his support in analyzing hydrocarbon contents, M. Jackson for his help on MPMS measurements at the Institute for Rock Magnetism (IRM) Minnesota and H. Stutzke for his kind introduction to the field site in Hänigsen. The authors are very much thankful to the editor M. Dekkers and an anonymous reviewer for their constructive comments to improve the original version of this manuscript. The financial support of the Deutsche Forschungsgemeinschaft (DFG) under the project contract AP 34/28-1, 2 is gratefully acknowledged.

References

Aldana M., Costanzo-Alvarez V. and Diaz M., 2003. Magnetic and mineralogical studies to characterize oil reservoirs in Venezuela. *The Leading Edge*, **22**, 526–529.

Aldana M., Costanzo-Álvarez V., Gómez L., González C., Díaz M., Silva P. and Rada M., 2011. Identification of magnetic minerals related to hydrocarbon authigenesis in venezuelan oil fields using an alternative decomposition of isothermal remanence curves. *Stud. Geophys. Geod.*, **55**, 343–358.

Bazylinski D.A. and Frankel R.B., 2003. Biologically controlled mineralization in prokaryotes. *Rev. Miner. Geochem.*, **54**, 217–247.

Bekins B.A., Godsy E.M. and Warren E., 1999. Distribution of microbial physiologic types in an aquifer contaminated by crude oil. *Microb. Ecol.*, **37**, 263–275.

Bloemendal J., King J.W., Hall F.R. and Doh S.J., 1992. Rock magnetism of late Neogene and Pleistocene deep-sea sediments: relations to sediment source, diagenetic process, and sediment lithology. *J. Geophys. Res.*, **97**, 4361–4375.

Blume H.P., Deller B., Leschber R., Paetz A. and Wilke B.M., 2000. *Handbuch der Bodenuntersuchung: Terminologie, Verfahrensvorschriften und Datenblätter - Physikalische, chemische, biologische Untersuchungsverfahren - Gesetzliche Regelwerk.* Wiley-VCH, Beuth, Weinheim, Germany (in German).

Chang L., Roberts A.P., TangY., Rainford B.D., Muxworthy A.R. and Chen, Q., 2008. Fundamental magnetic parameters from pure synthetic greigite (Fe3S4). *J. Geophys. Res.*, **113**, B06104.

Cochran W.G., 1950. Estimation of bacterial densities by means of the "most probable number". *Biometrics*, **6**, 105–116.

Díaz M., Aldana M., Jiménez S.M., Sequera P. and Costanzo-Alvarez V., 2006. EPR and EOM studies in well samples from some Venezuelan oil fields: correlation with magnetic authigenesis. *Física del Petróleo Revista Mexicana de Fisica*, **52**, 63–65.

Evans M.E. and Heller F., 2003. *Environmental Magnetism.* Elsevier, Amsterdam, The Netherlands.

Fischer W.R., 1988. Microbiological reactions of iron in soils. In: Stucki J.W., Goodman B.A. and Schwertmann U. (Eds.), *Iron in Soils and Clay Minerals*. Reidel, Dordrecht, The Netherlands, 715–749.

Gautam P., Blaha U. and Appel E., 2005. Magnetic susceptibility of dust-loaded leaves as a proxy for traffic-related heavy metal pollution in Kathmandu city, Nepal. *Atmos. Environ.*, **39**, 2201–2211.

Grimley D.A., Arruda N.K. and Bramstedt M.W., 2004. Using magnetic susceptibility to facilitate more rapid reproducible and precise delineation of hydric soils in the Midwest USA. *Catena*, **58**, 183–213.

Grimley D.A. and Arruda N.K., 2007. Observations of magnetite dissolution in poorly drained soils. *Soil Sci.*, **172**, 968–982.

Grimley D.A. and Vepraskas M.J., 2000. Magnetic susceptibility for use in delineating hydric soils. *Soil Sci. Soc. Am. J.*, **64**, 2174–2180.

Guzmán O., Costanzo-Álvarez V., Aldana M. and Díaz M., 2011. Study of magnetic contrasts applied to hydrocarbon exploration in the Maturín Sub-Basin (eastern Venezuela). *Stud. Geophys. Geod.*, **55**, 359–376.

Hanesch M. and Scholger R., 2002. Mapping of heavy metal loadings in soils by means of magnetic susceptibility measurements. *Environ. Geol.*, **42**, 857–870.

Hegler F., Posth N.R., Jiang J. and Kappler A., 2008. Physiology of phototrophic iron(II)-oxidizing bacteria: Implications for modern and ancient environments. *FEMS Microbiol. Ecol.*, **66**, 250–260.

Kao C.M., Chen S.C., Liu J.K. and Wang Y.S., 2001. Application of microbial enumeration technique to evaluate the occurrence of natural bioremediation. *Water Res.*, **35**, 1951–1960.

Kapička A., Jordanova N., Petrovský E. and Ustjak S., 2000. Magnetic stability of power-plant fly ash in different soil solutions. *Phys. Chem. Earth*, **25**, 431–436.

Kapička A., Petrovský E., Ustjak S. and Macháčková K., 1999. Proxy mapping of fly-ash pollution of soils around a coal-burning power plant: a case study in the Czech Republic. *J. Geochem. Explor.*, **66**, 291–297.

Kappler A. and Straub K.L., 2005. Geomicrobiological cycling of iron. *Rev. Miner. Geochem.*, **59**, 85–108.

Klee J.A., 1993. A computer program for the determination of most probable number and its confidence limits. *J. Microbiol. Methods*, **18**, 91–98.

Krs M., Novák F., Krsová M., Pruner P., Kouklíková L. and Jansa J., 1992. Magnetic properties and metastability of greigite-smythite mineralization in brown-coal basins of the Krušné hory Piedmont, Bohemia. *Phys. Earth Planet. Inter.*, **70**, 273–287.

Kruiver P.P. and Passier H.F., 2001. Coercivity analysis of magnetic phases in sapropel S1 related to variations in redox conditions, including an investigation of the S ratio. *Geochem. Geophys. Geosyst.*, **2**, 2001GC000181.

Liu J., Zhu R., Roberts A.P., Li S. and Chang J.-H., 2004. High resolution analysis of early diagenetic effects on magnetic minerals in post-middle-Holocene continental shelf sediments from the Korea Strait. *J. Geophys. Res.*, **109**, DOI: 10.1029/2003JB002813.

Liu Q.S., Liu Q.S., Chan L.S., Yang T., Xia X.H. and Tongjin C., 2006. Magnetic enhancement caused by hydrocarbon migration in the Mawangmiao Oil Field, Jianghan Basin, China. *J. Pet. Sci. Eng.*, **53**, 25–33.

Lovley D.R., Stolz J.F., Nord. G.L. and Phillips E.J.P., 1987. Anaerobic production of magnetite by a dissimilatory ironreducing microorganism. *Nature*, **330**, 252–254.

Lovley D.R., Baedecker M.J., Lonergan D.J., Cozzarelli J.M., Phillips E.J.P. and Siegel D.J., 1989. Oxidation of aromatic contaminants coupled to microbial iron reduction. *Nature*, **339**, 297–300.

Lovley D.R. and Anderson R.T., 2000. Influence of dissimilatory metal reduction on fate of organic and metal contaminants in the subsurface. *Hydrogeol. J.*, **8**, 77–88.

Maher B.A., 1986. Characterization of soils by mineral magnetic measurements. *Phys. Earth. Planet. Inter.*, **42**, 76–92.

Maher B.A., 1991. Inorganic formation of ultrafine-grained magnetite. In: Frankel R.B. and Blakemore R.P. (Eds.), *Iron Biominerals*. Plenum, New York, 179–191.

Maher B.A., 1998. Magnetic properties of modern soils and Quarternary loessic paleosols: Paleoclimatic implications. *Palaeogeogr. Palaeoclimatol. Palaeoecol.*, **137**, 25–54.

Martins C.C., Mahiques M.M., Bícego M.C., Fukumoto M.M. and Montone R.C., 2007. Comparison between anthropogenic hydrocarbons and magnetic susceptibility in sediment cores from the Santos Estuary, Brazil. *Mar. Pollut. Bull.*, **54**, 240–246.

Moeslund L., Thamdrup B. and Jørgensen B.B., 1994. Sulfur and iron cycling in coastal sediment: radiotracer studies and seasonal dynamics. *Biogeochem.*, **27**, 129–152.

Morris W.A., Versteeg J.K., Marvin C.H., McCarry B.E. and Rukavina N.A., 1994. Preliminary comparisons between magnetic susceptibility and polycyclic aromatic hydrocarbon content in sediments from Hamilton Harbour, Western Lake Ontario. *Sci. Tot. Environ.*, **152**, 153–160.

Muxworthy A.R., Matzka J. and Petersen N., 2001. Comparison of magnetic parameters of urban atmospheric particulate matter with pollution and meteorological data. *Atmos. Environ.*, **35**, 4379–4386.

Petrovský E. and Ellwood B.B., 1999. Magnetic monitoring of air-, land-, and water-pollution. In: Maher B.A. and Thompson R. (Eds.), *Quaternary Climates, Environments and Magnetism*. Cambridge University Press, Cambridge, U.K., 279–322.

Raven K.P., Jain A. and Loeppert R.H., 1998. Arsenite and arsenate adsorption on ferrihydrite: Kinetics, equilibrium, and adsorption envelopes. *Environ. Sci. Technol.*, **32**, 344–349.

Rijal M.L., Appel E., Petrovský E. and Blaha U., 2010. Change of magnetic properties due to fluctuations of hydrocarbon contaminated groundwater in unconsolidated sediments. *Environ. Pollut.*, **158**, 1756–1762.

Roden E.E. and Zachara J.M., 1996. Microbial reduction of crystalline iron(III) oxides: Influence of oxide surface area and potential for cell growth. *Environ. Sci. Technol.*, **30**, 1618–1628.

Rossello-Mora R.A., Caccavo F., Osterlehner K., Springer N., Spring S., Schüler D., Ludwig W., Amann R., Vanncanneyt M. and Schleifer K.H., 1995. Isolation and taxonomic characterization of a halotolerant, facultatively iron-reducing bacterium. *Syst. Appl. Microbiol.*, **17**, 569–573.

Salama I.A., Koch G.G. and Tolley, H.D., 1978. On the estimation of the most probable number in a serial dilution technique.*Commun. Stat. Theor. Methodol.*, **A7**, 1267–1281.

Spiteri C., Kalinski V., Rösler W., Hoffmann V., Appel E. and MAGPROX Team., 2005. Magnetic screening of a pollution hotspot in the Lausitz area, Eastern Germany: correlation analysis between magnetic proxies and heavy metal contamination in soils. *Environ. Geol.*, **49**, 1–9.

Stookey L.L., 1970. Ferrozine - A New Spectrophotometric Reagent for Iron. *Anal. Chem.*, **42**, 779–781.

Straub K.L., Kappler A. and Schink B., 2005. Enrichment and isolation of ferric-iron- and humic-acid-reducing bacteria. *Methods Enzymol.*, **397**, 58–77.

Straub K.L., Schönhuber W.A., Buchholz-Cleven B.E. and Schink B., 2004. Diversity of ferrous iron-oxidizing, nitrate-reducing bacteria and their involvement in oxygen-independent iron cycling. *Geomicrobiol. J.*, **21**, 371–378.

Strzyszcz Z. and Magiera T., 1998. Magnetic susceptibility and heavy metals contamination in soils of Southern Poland. *Phys. Chem. Earth*, **23**, 1127–1131.